Supplemental Material for:

Fight not flight: parasites drive the bacterial evolution of resistance, not escape

Published in: The American Naturalist

Michael Blazanin[1,2,*], Jeremy Moore[3], Sydney Olsen[1], and Michael Travisano[1,4]

[1]Department of Ecology, Evolution, and Behavior, University of Minnesota, Saint Paul, MN, USA

[2]Department of Ecology and Evolutionary Biology, Yale University, New Haven, CT, USA

[3]Department of Molecular, Cellular and Developmental Biology, Yale University, New Haven, CT, USA

[4]Biotechnology Institute, University of Minnesota, Minneapolis, MN, 55108, USA

*Corresponding author, email: mikeblazanin@gmail.com

Supplementary Materials

Repeated passages

Table S1. Repeated Passages Due to Sampling. During experimental evolution seven transfers failed to show growth in at least one treatment after 24 hours, likely due to sampling effects of the low-density cell front. In these instances, a new set of plates was re-inoculated from the previous plates, which had been stored at 4C.

Experiment	Replicate Population	Transfer
Less favorable for phage growth	A	2
Less favorable for phage growth	B	2
Less favorable for phage growth	B	6
Less favorable for phage growth	B	7
More favorable for phage growth	C	1
More favorable for phage growth	D	1
More favorable for phage growth	D	2

Supplemental Material (not copyedited or formatted) for: Michael Blazanin, Jeremy Moore, Sydney Olsen, Michael Travisano. 2025. "Fight Not Flight: Parasites Drive the Bacterial Evolution of Resistance, Not Escape."
The American Naturalist 205(2). DOI: https://doi.org/10.1086/733414.

Evolved growth

During experimental evolution, bacteria may have adapted their growth characteristics and life history traits to the different treatments. Alternatively, these traits may have evolved following trade-offs with other traits that were under selection, like resistance to phages or dispersal in soft agar. To measure growth characteristics, we collected growth curves of evolved isolates from the final timepoint in liquid media. Each isolate was grown in their experimental evolution environment ("original"), as well as an environment with all nutrients doubled in concentration ("rich"). This rich media was included to possibly reveal cases when bacteria had evolved growth costs due to trade-offs with dispersal or resistance that had then been ameliorated by compensatory mutations. By doubling the nutrients, we hypothesized this may reveal any costs of evolution hidden by compensatory mutations.

Growth curves were computationally characterized, with computational findings manually validated, as described below. In particular, we identified the following traits:

- Maximum per-capita growth rate (r)
- Lag time (time when maximum per-capita growth first exceeded 0.5/hr, or 0.4/hr when 0.5 was never reached)
- Time when a diauxic shift occurred, if any (k_t)
- Density when a diauxic shift occurred, if any (k)
- Deceleration parameter as bacterial density approaches diauxic shift (v)

There was no significant effect of parasite distribution or evolved resistance on maximum per-capita growth rate (Fig S1, Table S2), and there were no notable effects in other growth characteristics (Figs S2, S3, S4, S5).

Methods for Quantifying Bacterial Growth in Liquid

To quantify bacterial growth in liquid, 4 µL of an overnight bacterial culture was added, in duplicate wells, to 146 µL of media in each well of a 96-well plate. Media included both the media experimental evolution was carried out in ("original"), and media with the concentrations of all components doubled from that ("rich"). This plate was shaken and incubated at the appropriate temperature overnight, with the OD600 read every 15 or 30 minutes.

Then, growth curve data was computationally characterized using gcplyr (Blazanin 2023) and fitted to determine isolates' lag time, maximum per-capita growth rate (r), and density and time when a diauxic shift was observed (k, k_t). The first half hour of data points were noisy, so they were excluded. Then, data was smoothed using a moving median of 3 points, followed by LOcally Etimated Scatterplot Smoothing (LOESS) with a span of either 1 hour or 6.94 hours. We identified the exponential start of logistic growth as the first point when the per-capita growth rate of the of the 1-hour LOESS-smoothed data exceeded 0.5/hour, or 0.4/hour when 0.5 was never reached. We identified the end of logistic growth as the first local minima in the derivative of the 6.94-hour LOESS-smoothed data. These criteria were manually verified as yielding time spans where the data reflected logistic growth, excluding any acclimation period at the beginning of the data, and any post-diauxic shift growth at the end of the data.

Supplemental Material (not copyedited or formatted) for: Michael Blazanin, Jeremy Moore, Sydney Olsen, Michael Travisano. 2025. "Fight Not Flight: Parasites Drive the Bacterial Evolution of Resistance, Not Escape."
The American Naturalist 205(2). DOI: https://doi.org/10.1086/733414.

We then fit the data in the logistic growth window with a differential equation for a modified form of logistic growth (Baranyi and Roberts 1994; Ram et al. 2019) (Equation 1). This form includes a deceleration parameter, v, to better fit bacterial density as it approaches carrying capacity. Here, N(t) denotes the density of bacteria at time t, r is the maximum per-capita growth rate, k is the carrying capacity, and v is the deceleration curve parameter.

$$\frac{dN}{dt} = rN\left(1 - \left(\frac{N}{k}\right)^{v}\right) \quad [1]$$

This differential equation has a closed-form solution (Ram et al. 2019) (Equation 2).

$$N(t) = \frac{k}{\left(1-\left(1-\left(\frac{k}{N_0}\right)^{v}\right)e^{-rvt}\right)^{\frac{1}{v}}} \quad [2]$$

Equation 2 was fitted to the raw unsmoothed data points in the logistic growth window. We then manually evaluated all wells with high fit error, excluding wells where the fit was poor. We extracted fitted maximum per-capita growth rates (r) and excluded any isolates where the standard deviation of r between technical replicates was greater than 0.12/hr (for less favorable phage growth condition) or 0.14/hr (for more favorable phage growth condition). These thresholds were chosen heuristically to exclude wells with large variation between replicates.

Supplemental Material (not copyedited or formatted) for: Michael Blazanin, Jeremy Moore, Sydney Olsen, Michael Travisano. 2025. "Fight Not Flight: Parasites Drive the Bacterial Evolution of Resistance, Not Escape."
The American Naturalist 205(2). DOI: https://doi.org/10.1086/733414.

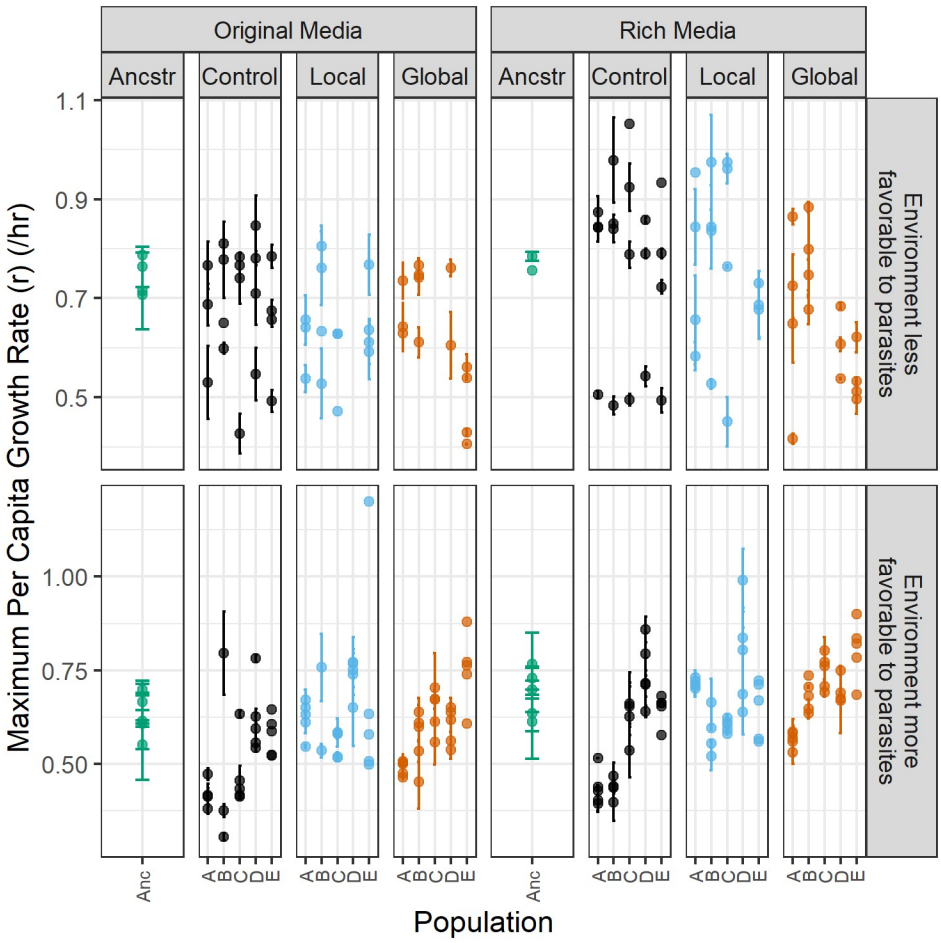

Figure S1. Evolved bacterial growth rates show no effects of parasite distribution. Bacterial isolates from the final transfer of experimental evolution were grown in liquid media containing the same (original) or double (rich) the nutrients as experienced during experimental evolution, quantifying their maximum per-capita growth rate. Each point represents the mean of two replicate wells containing the same isolate, with isolates from the same population stacked vertically, and error bars denoting the standard deviation between replicate wells. Note the difference in y-axis scales due to incubation and media differences between the experiment more favorable for phage growth and the experiment less favorable for phage growth. Less favorable phage growth local population D and global population C were contaminated during experimental evolution and excluded.

Table S2. Statistical tests for differences in maximum per-capita growth rate. Mixed effects modeling of maximum per-capita growth rate was carried out using lmer. As a null model, we included random effects for the population and for the batch date. We then compared this null model to models with fixed effects with a Kenward-Roger approximate F-test. We included a fixed effect for treatment [ancestor, control, local, or global], a fixed effect for resistance [none, partial (EOP above detection limit but below 0.1), or complete (EOP below detection limit)], or both. No tests were significant, indicating that neither treatment nor resistance were significantly associated with evolved maximum per-capita growth rate in either condition or media.

Experiment	Media	Fixed Effects	Approximate F-Statistic	p-value
Less favorable for phage growth	Original	Treatment	1.57	0.26
Less favorable for phage growth	Rich	Treatment	2.64	0.09
Less favorable for phage growth	Original	Resistance	2.49	0.11
Less favorable for phage growth	Rich	Resistance	2.56	0.11
Less favorable for phage growth	Original	Treatment + Resistance	2.96	0.07
Less favorable for phage growth	Rich	Treatment + Resistance	1.30	0.33
More favorable for phage growth	Original	Treatment	2.03	0.16
More favorable for phage growth	Rich	Treatment	1.25	0.34
More favorable for phage growth	Original	Resistance	0.80	0.46
More favorable for phage growth	Rich	Resistance	0.35	0.71
More favorable for phage growth	Original	Treatment + Resistance	1.24	0.34
More favorable for phage growth	Rich	Treatment + Resistance	0.72	0.62

Supplemental Material (not copyedited or formatted) for: Michael Blazanin, Jeremy Moore, Sydney Olsen, Michael Travisano. 2025. "Fight Not Flight: Parasites Drive the Bacterial Evolution of Resistance, Not Escape."
The American Naturalist 205(2). DOI: https://doi.org/10.1086/733414.

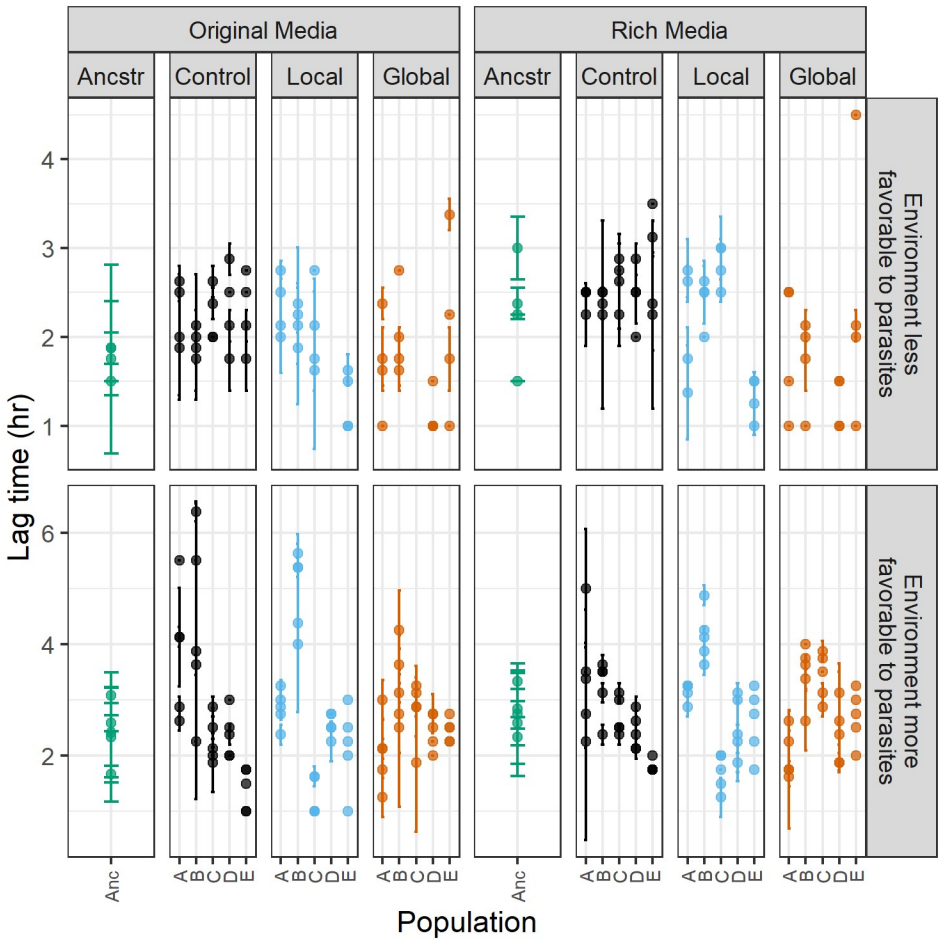

Figure S2. Evolution of lag time. Growth curves of ancestral and evolved bacterial isolates were collected in liquid media containing the same (original) or double (rich) the nutrients as experienced during experimental evolution. Each point represents the mean of two replicate wells containing the same isolate, with isolates from the same population stacked vertically, and error bars denoting the standard deviation between replicate wells. Note the difference in y-axis scales due to incubation and media differences between the experiment more favorable for phage growth and the experiment less favorable for phage growth. Less favorable phage growth local population D and global population C were contaminated during experimental evolution and excluded.

Supplemental Material (not copyedited or formatted) for: Michael Blazanin, Jeremy Moore, Sydney Olsen, Michael Travisano. 2025. "Fight Not Flight: Parasites Drive the Bacterial Evolution of Resistance, Not Escape."
The American Naturalist 205(2). DOI: https://doi.org/10.1086/733414.

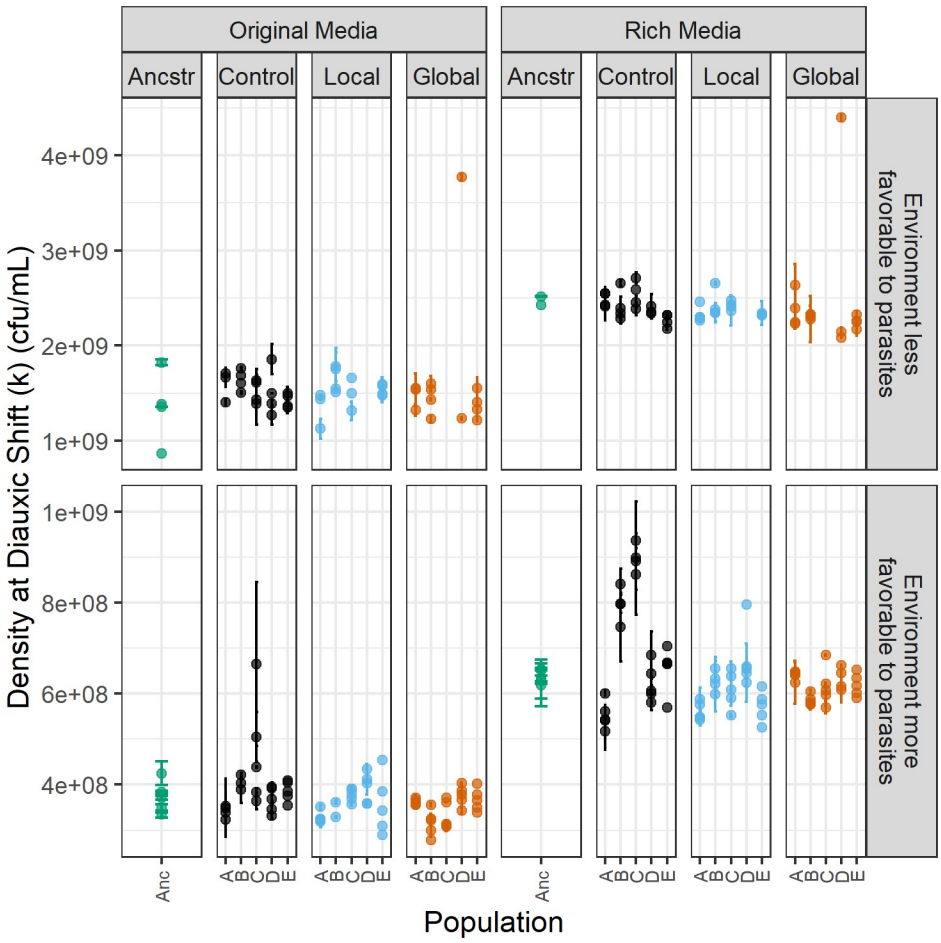

Figure S3. Evolution of diauxic shift density. Growth curves of ancestral and evolved bacterial isolates were collected in liquid media containing the same (original) or double (rich) the nutrients as experienced during experimental evolution. Each point represents the mean of two replicate wells containing the same isolate, with isolates from the same population stacked vertically, and error bars denoting the standard deviation between replicate wells. Points that are outliers with high diauxic shift densities were curves where the bacteria did not undergo a computationally identifiable diauxic shift. Note the difference in y-axis scales due to incubation and media differences between the experiment more favorable for phage growth and the experiment less favorable for phage growth. Less favorable phage growth local population D and global population C were contaminated during experimental evolution and excluded.

Supplemental Material (not copyedited or formatted) for: Michael Blazanin, Jeremy Moore, Sydney Olsen, Michael Travisano. 2025. "Fight Not Flight: Parasites Drive the Bacterial Evolution of Resistance, Not Escape."
The American Naturalist 205(2). DOI: https://doi.org/10.1086/733414.

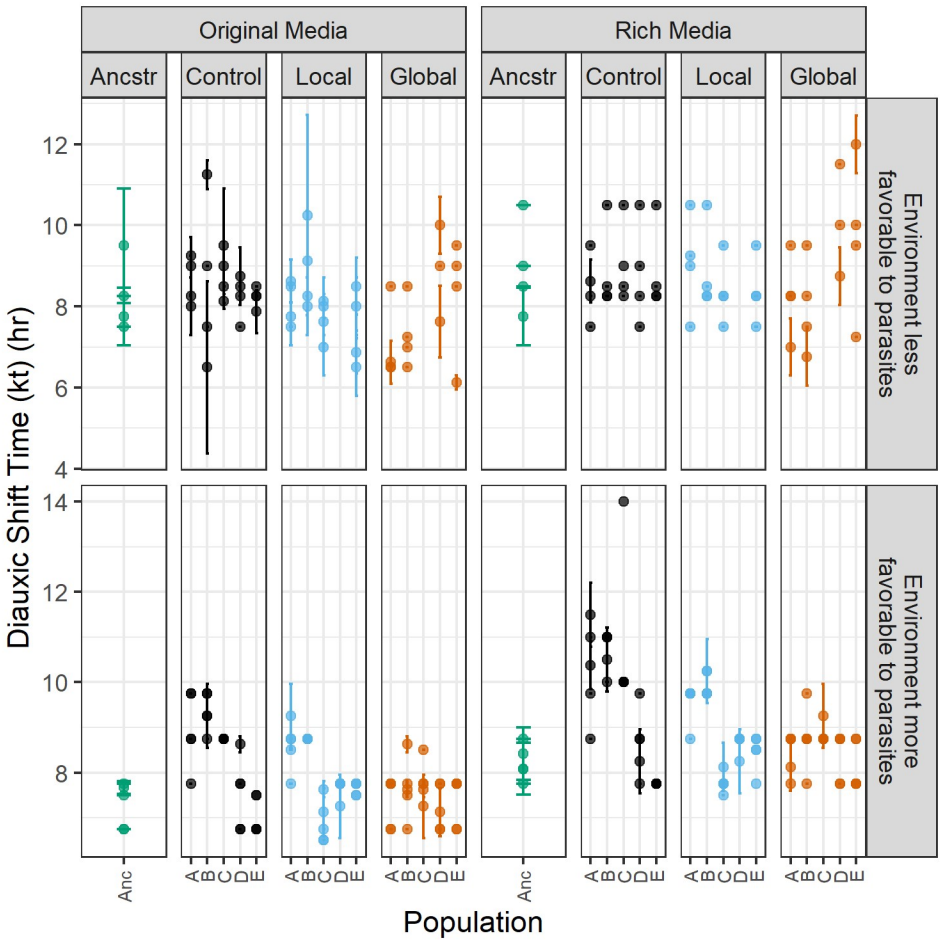

Figure S4. Evolution of diauxic shift timing. Growth curves of ancestral and evolved bacterial isolates were collected in liquid media containing the same (original) or double (rich) the nutrients as experienced during experimental evolution. Each point represents the mean of two replicate wells containing the same isolate, with isolates from the same population stacked vertically, and error bars denoting the standard deviation between replicate wells. Note the difference in y-axis scales due to incubation and media differences between the experiment more favorable for phage growth and the experiment less favorable for phage growth. Less favorable phage growth local population D and global population C were contaminated during experimental evolution and excluded.

Supplemental Material (not copyedited or formatted) for: Michael Blazanin, Jeremy Moore, Sydney Olsen, Michael Travisano. 2025. "Fight Not Flight: Parasites Drive the Bacterial Evolution of Resistance, Not Escape."
The American Naturalist 205(2). DOI: https://doi.org/10.1086/733414.

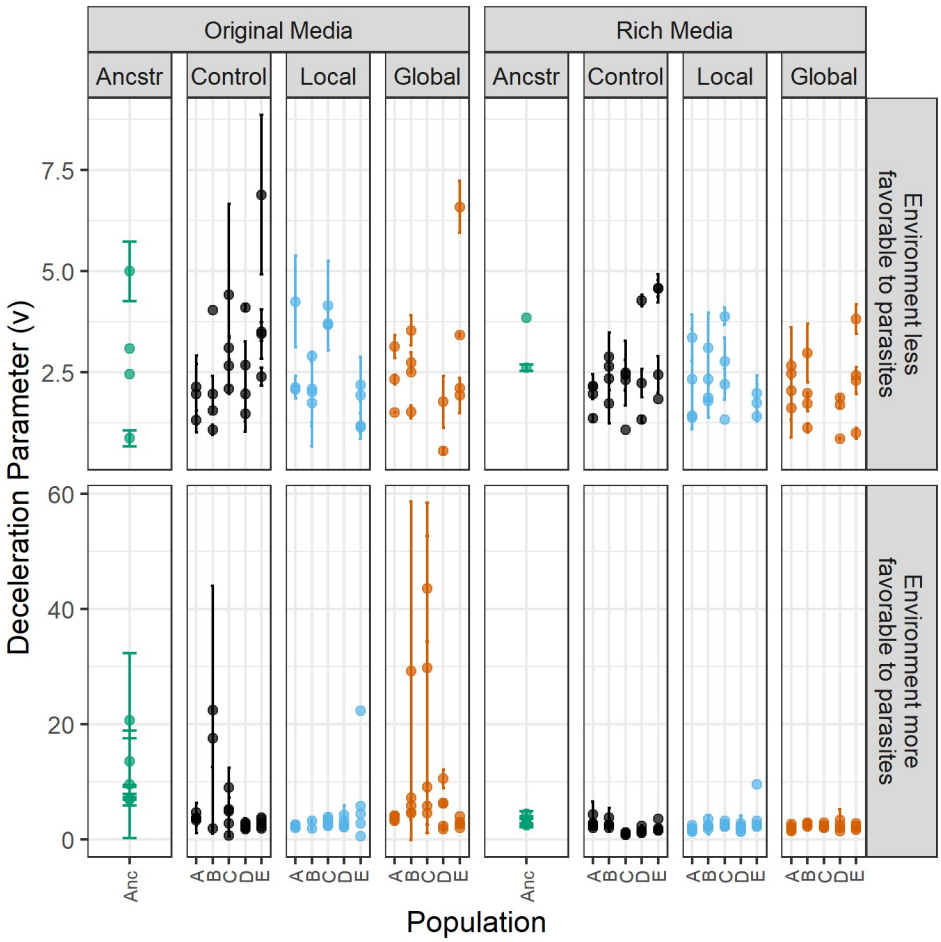

Figure S5. Evolution of deceleration parameter. Growth curves of ancestral and evolved bacterial isolates were collected in liquid media containing the same (original) or double (rich) the nutrients as experienced during experimental evolution. Each point represents the mean of two replicate wells containing the same isolate, with isolates from the same population stacked vertically, and error bars denoting the standard deviation between replicate wells. Note the difference in y-axis scales due to incubation and media differences between the experiment more favorable for phage growth and the experiment less favorable for phage growth. Less favorable phage growth local population D and global population C were contaminated during experimental evolution and excluded.

Supplemental Material (not copyedited or formatted) for: Michael Blazanin, Jeremy Moore, Sydney Olsen, Michael Travisano. 2025. "Fight Not Flight: Parasites Drive the Bacterial Evolution of Resistance, Not Escape."
The American Naturalist 205(2). DOI: https://doi.org/10.1086/733414.

Relationships among evolved traits

To identify relationships among evolved traits in bacterial isolates, including dispersal, resistance to phages, and growth characteristics, we merged all three datasets characterizing the ancestral and evolved isolates. We then excluded any isolates with missing data. We carried out checks for univariate normalcy of all variables, and transformed some variables for improved normalcy: resistance was -$\log_{10}$(Efficiency of Plaquing), and diauxic shift density (k) was $\log_{10}$(k). Data from the relatively slower growing phage condition-evolved bacteria was multivariate normal, while data from the relatively faster growing phage condition-evolved bacteria was not multivariate normal. Data was scaled and centered and principal component analyses were run.

Generally, multivariate analyses reveal that growth traits were highly correlated between the original and rich medias within a condition (relatively slower growing phage or relatively faster growing phage) (Fig S6). In contrast, growth traits tended to have inconsistent relationships across the two conditions. We observe that global treatment isolates have most diverged from the ancestor in relatively slower growing phage conditions, while control treatment populations have most diverged from the ancestor in relatively faster growing phage conditions (Fig S7).

Previous work has also commonly found relationships between evolved bacterial traits, something we failed to consistently find in our data (Figs S6, S7). For instance, past work has documented tradeoffs between phage resistance and competitive ability (Brockhurst et al. 2004), dispersal and growth rate (Fraebel et al. 2017), or found that evolution with phages can constrain adaptation to the abiotic environment (Koskella et al. 2011; Scanlan et al. 2015). That said, some studies have also failed to find relationships between phage resistance, bacterial motility, and growth, as we did (Koskella et al. 2011). Further work is needed to disentangle the factors driving these differences between studies.

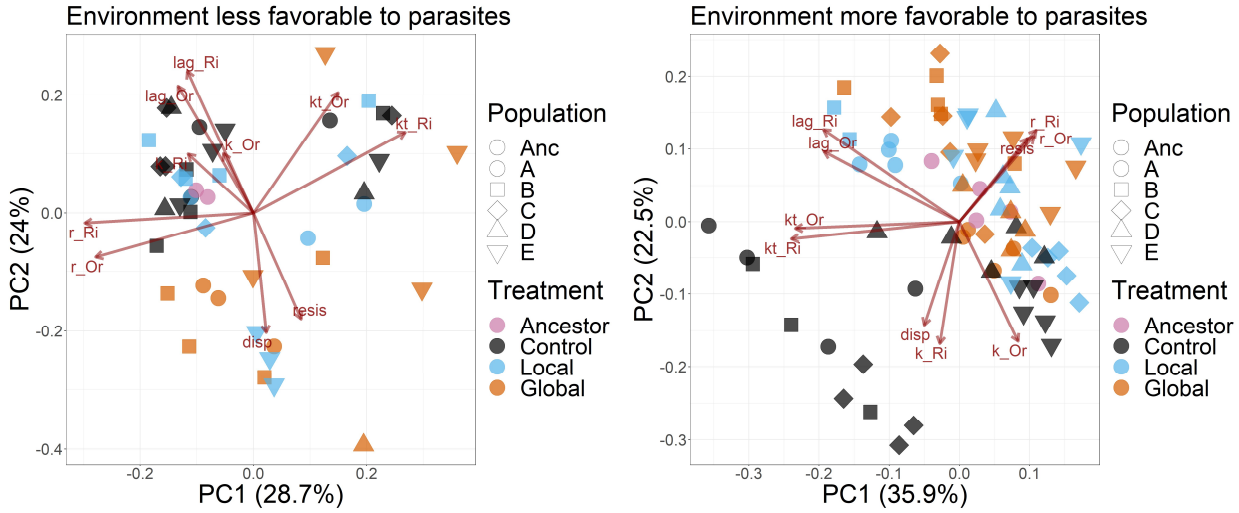

Figure S6. Correlation biplot showing multivariate evolution of bacterial traits. Data from growth curves, dispersal, and resistance assays were combined, normalized, and principal component analyses

Supplemental Material (not copyedited or formatted) for: Michael Blazanin, Jeremy Moore, Sydney Olsen, Michael Travisano. 2025. "Fight Not Flight: Parasites Drive the Bacterial Evolution of Resistance, Not Escape."
The American Naturalist 205(2). DOI: https://doi.org/10.1086/733414.

were run. Each point corresponds to a single isolate. Shown is a correlation biplot for each of the two conditions, where the angles between two variable vectors reflects their correlation. resis is $-\log_{10}$(Efficiency of Plaquing) and disp is dispersal rate. Growth characteristics of lag time (lag), maximum per-capita growth rate (r), the density at diauxic shift (k), and the time of diauxic shift (kt) were measured in media containing the original concentration of nutrients as used in experimental evolution (Or), and rich media containing double the nutrient concentration (Ri). Note that there are incubation and media differences between the environment more favorable to phage and the environment less favorable to phage.

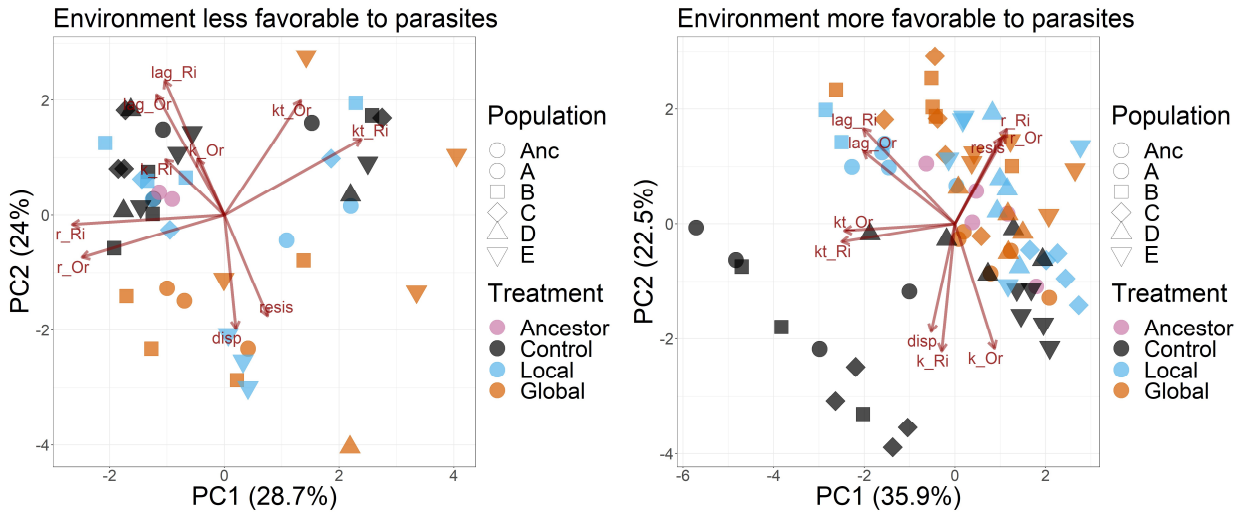

Figure S7. Distance biplot showing multivariate evolution of bacterial traits. Data from growth curves, dispersal, and resistance assays were combined, normalized, and principal component analyses were run. Each point corresponds to a single isolate. Shown is a distance biplot for each of the two conditions, where distances among isolates approximate their Euclidean distance in multidimensional space. resis is $-\log_{10}$(Efficiency of Plaquing) and disp is dispersal rate. Growth characteristics of lag time (lag), maximum per-capita growth rate (r), the density at diauxic shift (k), and the time of diauxic shift (kt) were measured in media containing the original concentration of nutrients as used in experimental evolution (Or), and rich media containing double the nutrient concentration (Ri). Note that there are incubation and media differences between the environment more favorable to phage and the environment less favorable to phage.

Supplemental Material (not copyedited or formatted) for: Michael Blazanin, Jeremy Moore, Sydney Olsen, Michael Travisano. 2025. "Fight Not Flight: Parasites Drive the Bacterial Evolution of Resistance, Not Escape."
The American Naturalist 205(2). DOI: https://doi.org/10.1086/733414.

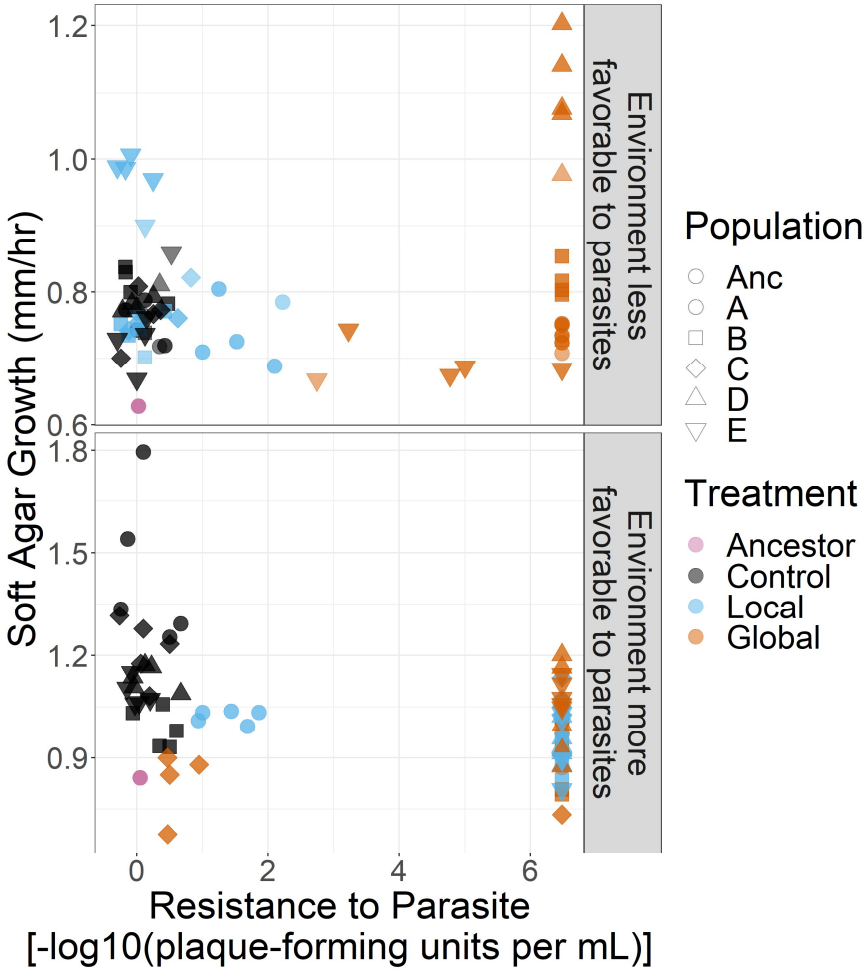

Figure S8. No consistent relationship between dispersal and resistance among evolved bacteria. We combined data from dispersal and resistance assays, then ran a linear mixed-effects model for each environment of dispersal with a random effect for population, and fixed effects for treatment (intercept) and the interaction of treatment and resistance (slope). In the less favorable environment for parasites, we find no slopes of dispersal against resistance that significantly vary from 0 (control $p = 0.39$, local $p = 0.91$, global $p = 0.45$). In the more favorable environment for parasites, we did find that the control treatment has a significant relationship between dispersal and resistance (control estimated slope -0.15, $p = 0.001$; local $p = 0.68$; global $p = 0.43$). However, given the extremely limited range of resistance in control isolates, this relationship is likely spurious. Note that there are incubation and media differences between the environment more favorable to phage and the environment less favorable to phage.

Supplemental Material (not copyedited or formatted) for: Michael Blazanin, Jeremy Moore, Sydney Olsen, Michael Travisano. 2025. "Fight Not Flight: Parasites Drive the Bacterial Evolution of Resistance, Not Escape."
The American Naturalist 205(2). DOI: https://doi.org/10.1086/733414.

Simulations parameterization

Table S3. Parameters and values used in simulations. The sources for each parameter value and range of parameter values are listed. The fitting or derivation of some values is listed in more detail below.

Parameter	Description	Resident Value	Invader Values	Source
D_N	Diffusion coefficient for bacteria	50 $\mu m^2/s$	N/A	(Cremer et al. 2019)
D_P	Diffusion coefficient for phage	0 or 40 $\mu m^2/s$	N/A	Below
D_R	Diffusion coefficient for resource	800 $\mu m^2/s$	N/A	(Cremer et al. 2019)
D_A	Diffusion coefficient for attractant	800 $\mu m^2/s$	N/A	(Cremer et al. 2019)
χ	Chemotactic sensitivity coefficient	315 $\mu m^2/s$	57 – 1770 $\mu m^2/s$	(Cremer et al. 2019)
c_R	Uptake rate of resource	2.25×10^{-14} mmol/cfu/s	$1 – 5 \times 10^{-14}$ mmol/cfu/s	Fitted, below
c_A	Uptake rate of attractant	4.17×10^{-16} mmol/cfu/s	$1.8 – 9.4 \times 10^{-16}$ mmol/cfu/s	(Cremer et al. 2019)
Y	Cell yield	1.229×10^{10} cfu/mmol	$0.873 – 1.733 \times 10^{10}$ cfu/mmol	Fitted, below
K_R	Michaelis-Menten constant for resource	5×10^{-5} mmol/mL	N/A	(Cremer et al. 2019)
K_A	Michaelis-Menten constant for attractant	1×10^{-6} mmol/mL	N/A	(Cremer et al. 2019)
i	Infection rate	1×10^{-12} infec/cell/mL/pfu/mL/s	$0.01 – 100 \times 10^{-12}$ infec/cell/mL/pfu/mL/s	(Paepe and Taddei 2006; Wang 2006; Heineman and Bull 2007; Shao and Wang 2008; Gallet et al. 2009; Turner et al. 2012; Lindberg et al. 2014)
b	Number of parasites produced per infection	30 pfu/infec	3 – 300 pfu/infec	(Josslin 1970; Reader and Siminovitch 1971; Paepe and Taddei 2006; Wang 2006; Heineman and Bull 2007; Gallet et al. 2009; Shao and Wang 2009; Turner et al. 2012; Lindberg et al. 2014)

D_P was set to zero because phage particles lack any active motility, and passive diffusion of viral particles through agar gel is very slow relative to the diffusion of nutrients and attractants, or diffusion and migration of bacteria. To ensure that our findings were not sensitive to this assumption, we also did all simulations with D_P = 40 $\mu m^2/s$ (Ping et al. 2020).

Y was approximated from the observed growth curve data (Fig S3), where bacterial cultures reached carrying capacity on the primary resource around 10^9 cfu/mL (in the richer media of the slower growing phage condition). Since that media contains 7.5 g/L glycerol (the primary carbon source, molar mass = 92.09 g/mol), this implies a yield of approximately 1.229×10^{10} cfu/mmol of glycerol. The range of invader values was set to include and exceed the variation we observed in carrying capacities in our experimental data.

c_R was approximated from the observed growth curve data (Fig S1), where bacteria doubled slightly slower than once per hour. For simplicity, we approximated the maximum bacterial growth rate (r) as 1 /hour. Given the known cell yield and primary carbon source concentration (above), this implies a resource uptake rate $c_R = \frac{r}{Y} = 2.25 \times 10^{-14}$ mmol/cfu/s. The range of invader values was set to include and exceed the variation we observed in maximum growth rate in our experimental data.

Simulation results

As described in the main text, we leveraged existing mathematical models of bacterial growth and dispersal to simulate bacterial evolution in the presence of different parasite spatial distributions across a wide range of bacterial trait values. Using *in silico* invasion experiments, we uncovered the fitness landscape between resistance and other bacterial traits. In the main text we report the fitness landscape between resistance and dispersal with three initial parasite distributions: none, gaussian-distributed (local), and uniformly-distributed (global) (Fig 6). Here, we include an additional "global" parasite distribution that uses a wider gaussian distribution, controlling for possible effects of gaussian vs uniform initial parasite distributions (Fig S9). We also report fitness landscapes between resistance and growth rate (Fig S10), yield (Fig S11), or attractant consumption (Fig S12). In addition, we explore the fitness landscape of bacterial mutations that alter the burst size of each phage infection (number of phage progeny produced per infection). Although burst size is conventionally considered a phage trait, here we model changes in burst size being determined by bacterial genotype, which could arise for example if burst size is altered via genotype-by-genotype interactions between the bacteria and phage (GxG). Specifically, we uncovered the landscapes between burst size and resistance (Fig S13), dispersal (Fig S14), growth rate (Fig S15), yield (Fig S16), and attractant consumption (Fig S17). Finally, in the main text we report the fitness landscape of resistance and dispersal under the assumption of no phage diffusion. Here, we include additional simulations where we relax that assumption, with D_P = 40 $\mu m^2/s$ (Ping et al. 2020) (Figs S9 – S17).

These fitness landscapes reveal that, in the absence of parasites, increased dispersal, growth rate, and yield are adaptive, while (as expected) resistance is neutral. In the presence of parasites, resistance becomes adaptive. In landscapes of resistance with growth rate and yield, this has the effect of making

Supplemental Material (not copyedited or formatted) for: Michael Blazanin, Jeremy Moore, Sydney Olsen, Michael Travisano. 2025. "Fight Not Flight: Parasites Drive the Bacterial Evolution of Resistance, Not Escape."
The American Naturalist 205(2). DOI: https://doi.org/10.1086/733414.

both resistance and the other trait adaptive. However, strikingly, in the landscape of resistance and dispersal, dispersal loses its fitness benefits, suggesting that the unique dynamics of resistance and dispersal evolution eliminate the benefits of dispersal in the presence of parasites. These patterns only become more pronounced when comparing local to global to global (gaussian) initial parasite distributions. In contrast to resistance, reduced burst size provides little fitness benefit to the bacteria, regardless of parasite spatial distribution. Finally, when phages are allowed to diffuse, the fitness landscapes become more similar between treatments with parasites added in different initial distributions, but the qualitative shape of the fitness landscapes does not change.

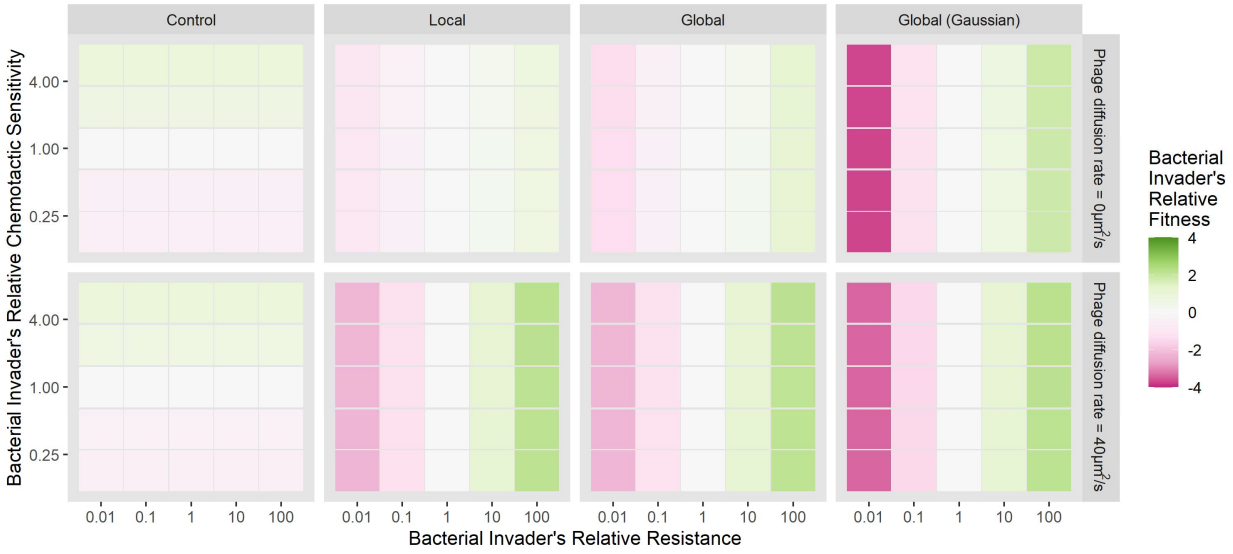

Fig S9. Parasite presence selects for host resistance and eliminates selection for host dispersal. *In silico* invasion experiments were carried out with a bacterial mutant that varied in resistance and chemotactic sensitivity relative to the resident bacterial population, both competing in the presence of one of four different initial parasite spatial distributions. Results are colored by invader fitness = $\log_{10}$(final invader frequency/final resident frequency). Resistance is defined as the reciprocal of infection rate (1/i).

Supplemental Material (not copyedited or formatted) for: Michael Blazanin, Jeremy Moore, Sydney Olsen, Michael Travisano. 2025. "Fight Not Flight: Parasites Drive the Bacterial Evolution of Resistance, Not Escape."
The American Naturalist 205(2). DOI: https://doi.org/10.1086/733414.

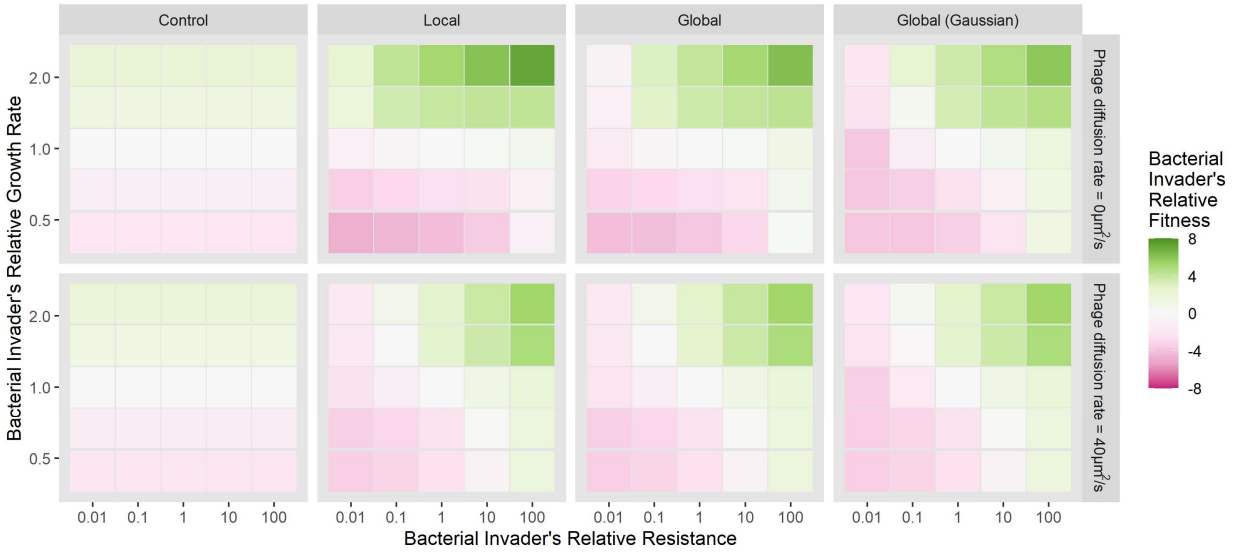

Fig S10. Parasite presence selects for host resistance and maintains selection for host growth rate. *In silico* invasion experiments were carried out with a bacterial mutant that varied in resistance and growth rate relative to the resident bacterial population, both competing in the presence of one of four different initial parasite spatial distributions. Results are colored by invader fitness = $\log_{10}$(final invader frequency/final resident frequency). Resistance is defined as the reciprocal of infection rate (1/i).

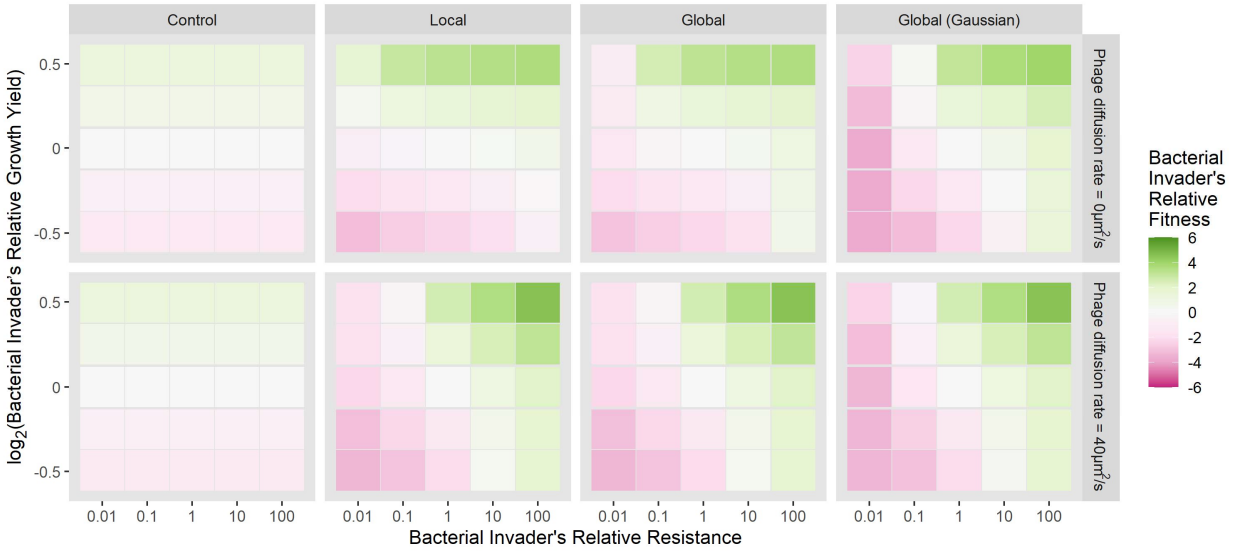

Fig S11. Parasite presence selects for host resistance and maintains selection for host growth yield. *In silico* invasion experiments were carried out with a bacterial mutant that varied in resistance and growth yield relative to the resident bacterial population, both competing in the presence of one of four different initial parasite spatial distributions. Results are colored by invader fitness = $\log_{10}$(final invader frequency/final resident frequency). Resistance is defined as the reciprocal of infection rate (1/i).

Supplemental Material (not copyedited or formatted) for: Michael Blazanin, Jeremy Moore, Sydney Olsen, Michael Travisano. 2025. "Fight Not Flight: Parasites Drive the Bacterial Evolution of Resistance, Not Escape."
The American Naturalist 205(2). DOI: https://doi.org/10.1086/733414.

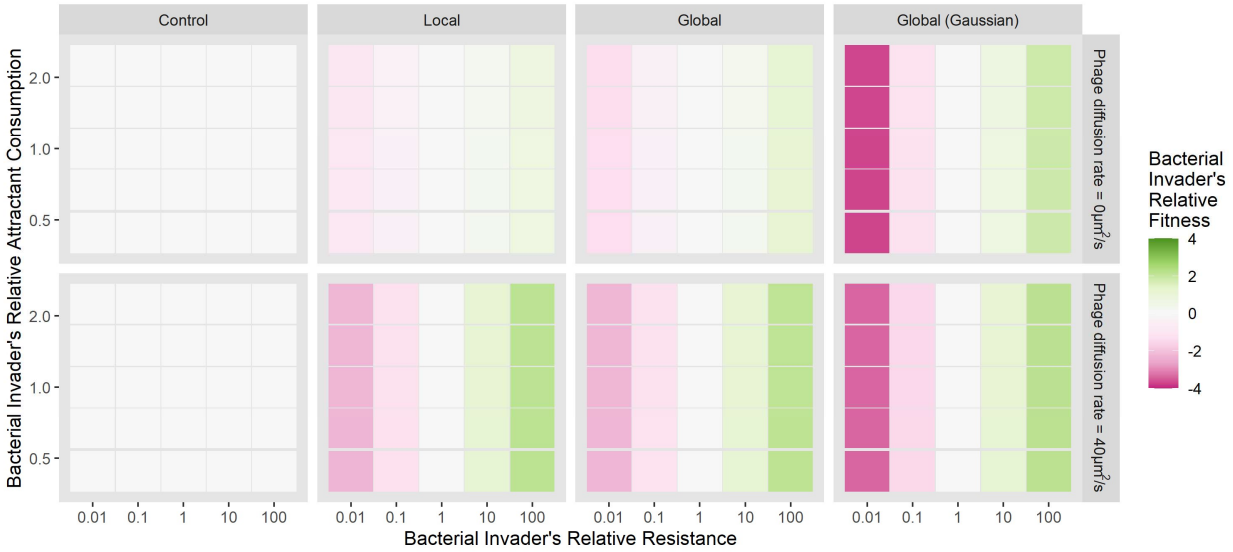

Fig S12. Parasite presence selects for host resistance with no effect on selection for host attractant consumption. *In silico* invasion experiments were carried out with a bacterial mutant that varied in resistance and attractant consumption rate relative to the resident bacterial population, both competing in the presence of one of four different initial parasite spatial distributions. Results are colored by invader fitness = $\log_{10}$(final invader frequency/final resident frequency). Resistance is defined as the reciprocal of infection rate (1/i).

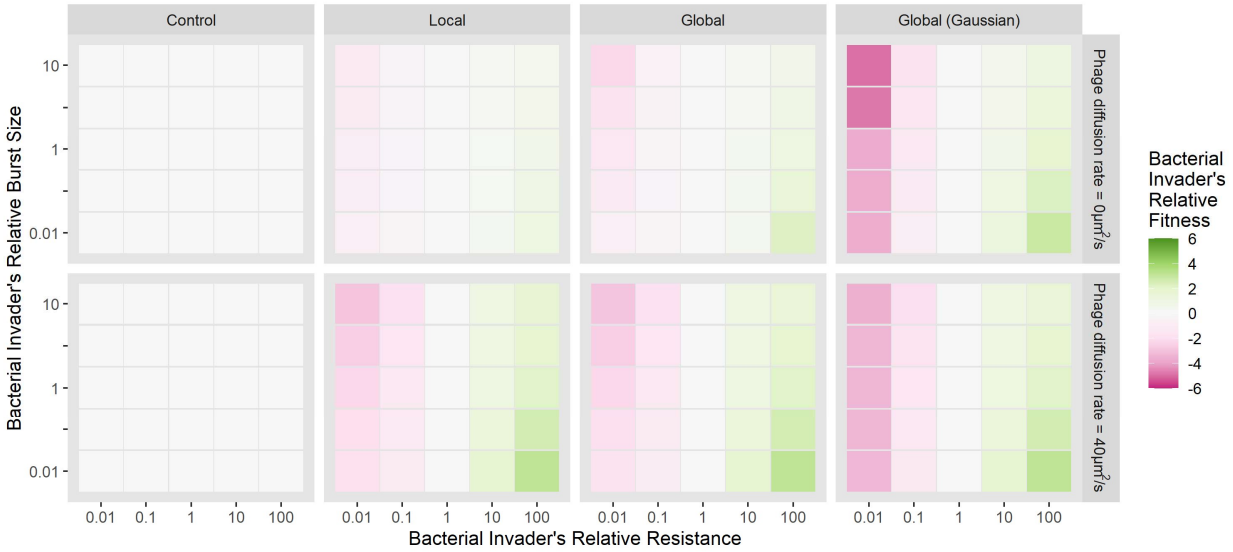

Fig S13. Parasite presence selects for host resistance but only weakly on burst size. *In silico* invasion experiments were carried out with a bacterial mutant that varied in resistance and the burst size of parasite infections relative to the resident bacterial population, both competing in the presence of one of four different initial parasite spatial distributions. Results are colored by invader fitness = $\log_{10}$(final invader frequency/final resident frequency). Resistance is defined as the reciprocal of infection rate (1/i).

Supplemental Material (not copyedited or formatted) for: Michael Blazanin, Jeremy Moore, Sydney Olsen, Michael Travisano. 2025. "Fight Not Flight: Parasites Drive the Bacterial Evolution of Resistance, Not Escape."
The American Naturalist 205(2). DOI: https://doi.org/10.1086/733414.

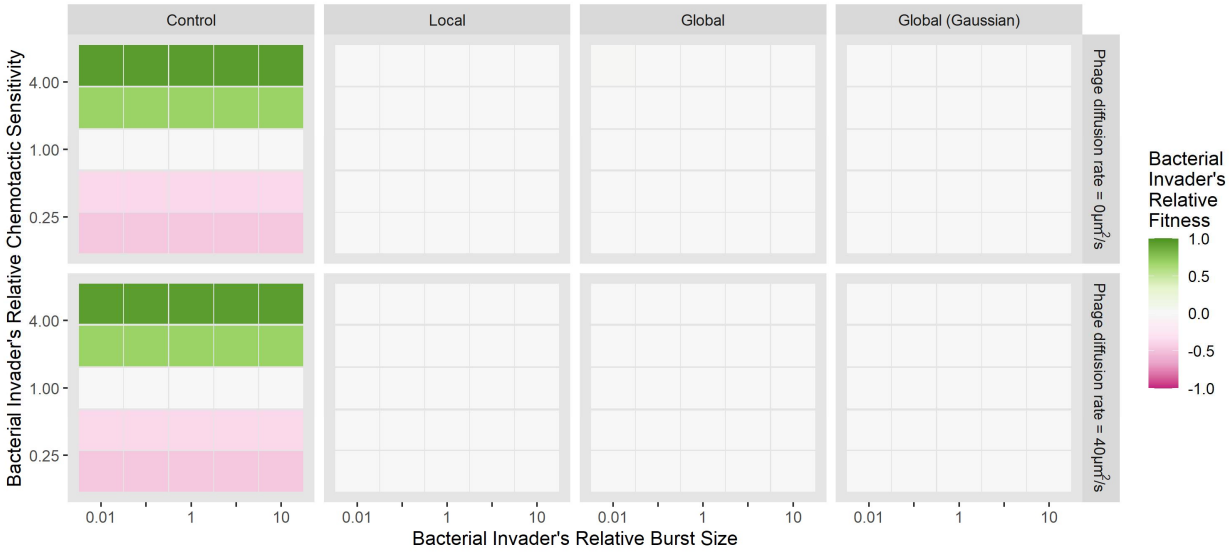

Fig S14. Chemotactic sensitivity is beneficial in the absence of parasites, but burst size is never beneficial. *In silico* invasion experiments were carried out with a bacterial mutant that varied in the burst size of parasite infections and chemotactic sensitivity relative to the resident bacterial population, both competing in the presence of one of four different initial parasite spatial distributions. Results are colored by invader fitness = $\log_{10}$(final invader frequency/final resident frequency).

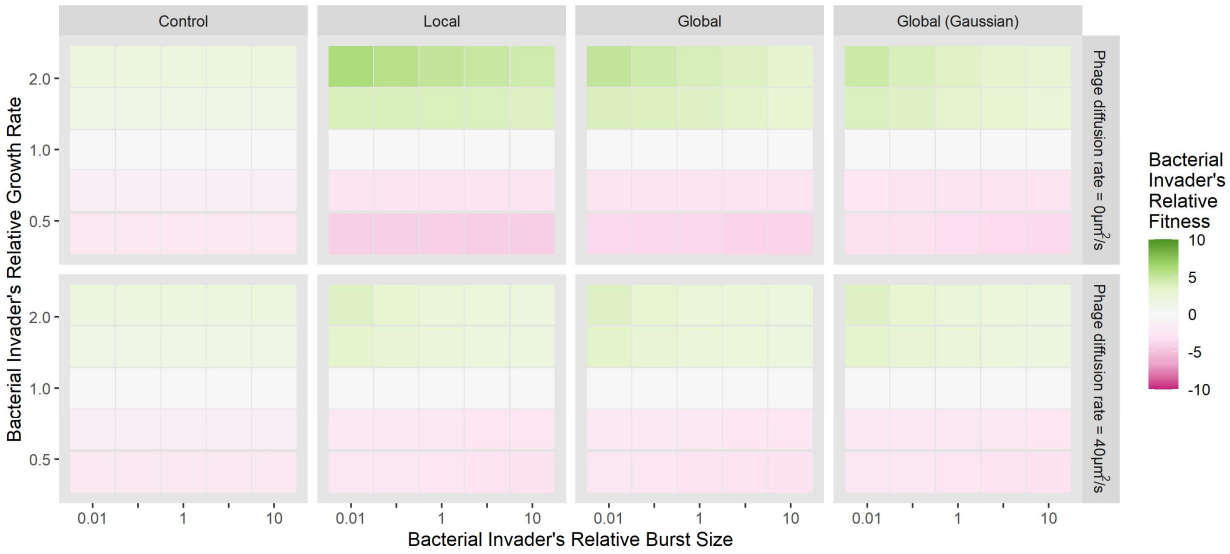

Fig S15. Growth rate is always beneficial, but burst size is weakly beneficial. *In silico* invasion experiments were carried out with a bacterial mutant that varied in the burst size of parasite infections and growth rate relative to the resident bacterial population, both competing in the presence of one of four different initial parasite spatial distributions. Results are colored by invader fitness = $\log_{10}$(final invader frequency/final resident frequency).

Supplemental Material (not copyedited or formatted) for: Michael Blazanin, Jeremy Moore, Sydney Olsen, Michael Travisano. 2025. "Fight Not Flight: Parasites Drive the Bacterial Evolution of Resistance, Not Escape."
The American Naturalist 205(2). DOI: https://doi.org/10.1086/733414.

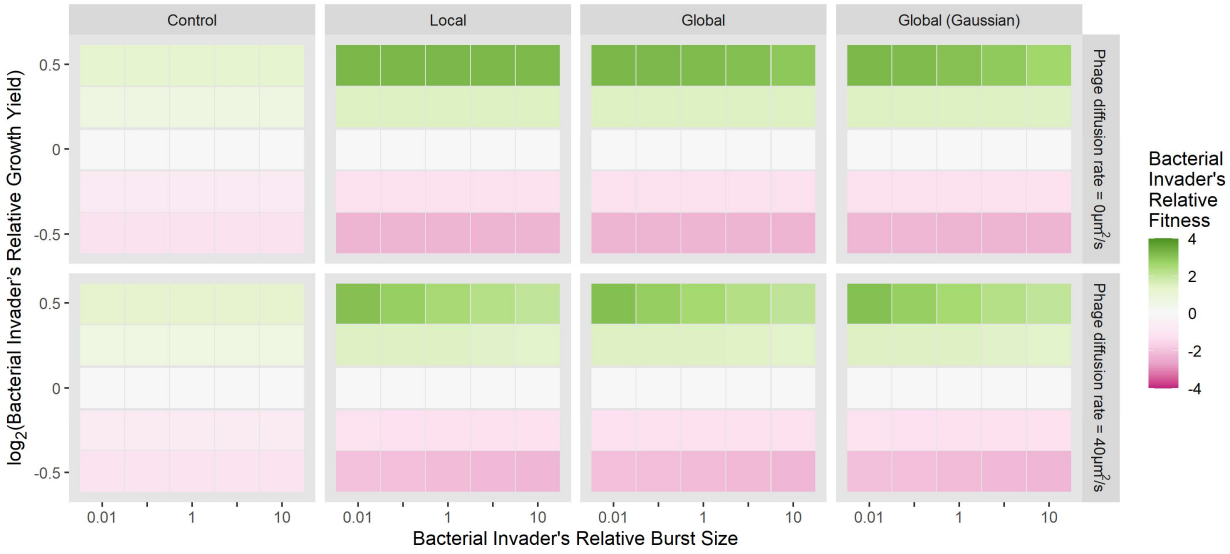

Fig S16. Yield is always beneficial while burst size is barely beneficial. *In silico* invasion experiments were carried out with a bacterial mutant that varied in the burst size of parasite infections and growth yield relative to the resident bacterial population, both competing in the presence of one of four different initial parasite spatial distributions. Results are colored by invader fitness = $\log_{10}$(final invader frequency/final resident frequency).

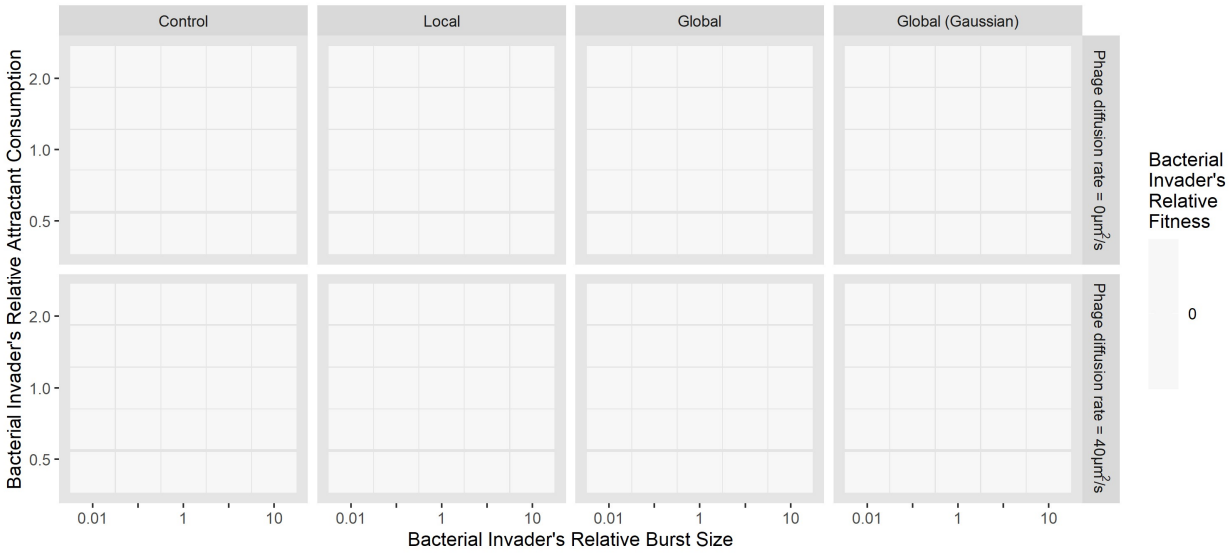

Fig S17. Neither attractant consumption nor burst size are beneficial. *In silico* invasion experiments were carried out with a bacterial mutant that varied in the burst size of parasite infections and attractant consumption rate relative to the resident bacterial population, both competing in the presence of one of four different initial parasite spatial distributions. Results are colored by invader fitness = $\log_{10}$(final invader frequency/final resident frequency).